Journal of Molecular Structure 1118 (2016) 117–123

Contents lists available at ScienceDirect

Journal of Molecular Structure

journal homepage: http://www.elsevier.com/locate/molstruc

Investigations on surface chemical analysis using X-ray photoelectron spectroscopy and optical properties of Dy^{3+}-doped $LiNa_3P_2O_7$ phosphor

K. Munirathnam [a], G.R. Dillip [b, **], Shivanand Chaurasia [c], S.W. Joo [b, ***], B. Deva Prasad Raju [d, *], N. John Sushma [e]

[a] Department of Physics, Sri Venkateswara University, Tirupati 517 502, India
[b] School of Mechanical Engineering, Yeungnam University, Gyeongsan 712 749, South Korea
[c] High Pressure & Synchrotron Radiation Physics Division, Bhabha Atomic Research Centre, Mumbai 400 085, India
[d] Department of Future Studies, Sri Venkateswara University, Tirupati 517 502, India
[e] Department of Biotechnology, Sri Padmavathi Women's University, Tirupati 517 502, India

ARTICLE INFO

Article history:
Received 13 January 2016
Received in revised form
4 April 2016
Accepted 4 April 2016
Available online 6 April 2016

Keywords:
Pyrophosphate
Solid-state reaction
X-ray photoelectron spectroscopy
White light

ABSTRACT

Near white-light emitting $LiNa_3P_2O_7{:}Dy^{3+}$ phosphors were prepared by a conventional solid-state reaction method. The orthorhombic crystal structure of the phosphors was confirmed using X-ray diffraction (XRD), and the valence states of the surface elements were determined from the binding energies of Li 1s, O 1s, Na 1s, P 2p, and Dy 3d by X-ray photoelectron spectroscopy (XPS). Attenuated total reflectance (ATR) - Fourier transform infrared (FT-IR) spectroscopy was employed to identify the pyrophosphate groups in the phosphors. Diffuse reflectance spectra (DRS) show the absorption bands of the Dy^{3+} ions in the host material. Intense blue (481 nm) and yellow (575 nm) emissions were obtained at an excitation wavelength of 351 nm and are attributed to the $^4F_{9/2} \rightarrow {}^6H_{15/2}$ and $^4F_{9/2} \rightarrow {}^6H_{13/2}$ transitions of Dy^{3+} ions, respectively. The combination of these two intense bands generates light emission in the near-white region of the chromaticity diagram.

1. Introduction

Over the past few years, there has been increasing demand for luminescent materials for a wide range of applications, including plasma display panels (PDPs), Hg-free lamps, liquid crystal display (LCD) backlights, and quickly commercializing solid-state lighting (SSL) sources [1,2]. SSL devices have several advantages for lighting like significant power savings, longer lifetime, higher luminous efficiency, and environmental friendliness compared to conventional incandescent or fluorescent lamps [3].

Phosphor-converted light-emitting diodes (pc-LEDs) have received great attention due to their stable color, good color reproducibility, and higher color rendering indexes compared to RGB (red, green, and blue) LEDs. SSL devices based on pc-LEDs are commercializing quickly, but they suffer from various disadvantages like a poor color-rendering index (CRI) and low stability of the color temperature (CCT) [4–6]. To overcome these weaknesses, researchers have made numerous efforts to develop single-phase phosphors for white light generation. Various approaches are used to obtain white light emission in a single-phase host. The four following approaches are mainly considered for single-host white-emitting phosphors [3,7]: (i) introducing a suitable rare-earth (RE) ion (Eu^{3+}, Dy^{3+}, etc.) into the appropriate single-phase host matrix [8,9]; (ii) combining different RE ions (Tm^{3+}/Dy^{3+}, $Eu^{2+}/Tb^{3+}/Mn^{2+}$, etc.) with various emissions (red, green, blue, or yellow) [10,11]; (iii) selective co-doping of ion pairs ($Ce^{3+} \rightarrow Mn^{2+}$, $Eu^{2+} \rightarrow Mn^{2+}$, etc.) via an energy transfer mechanism [12,13]; and (iv) inducing appropriate defects in the luminescent materials (defect-related emissions) [14].

A suitable host matrix and dopant ion is important for obtaining a single-phase white-lighting phosphor. Phosphate-based phosphors are an important family of luminescent materials because of their excellent properties, such as a large band gap, high absorption

---

* Corresponding author.
** Corresponding author.
*** Corresponding author.

E-mail addresses: dillip.ngr@gmail.com (G.R. Dillip), swjoo@yu.ac.kr (S.W. Joo), drdevaprasadraju@gmail.com (B. Deva Prasad Raju).

http://dx.doi.org/10.1016/j.molstruc.2016.04.004

of PO_4^{3-} in the UV region (300–400 nm), cheaper raw materials, simple synthesis conditions, high thermal and chemical stability, and exceptional optical damage threshold [9,15]. Phosphate-based phosphors are a good host matrix for RE ion transitions. The interaction between the RE ions is weak in these matrices because the RE ions are separated from each other by the phosphate groups [16]. Therefore, one can expect good optical properties from these materials.

Among the various lanthanide ions, trivalent dysprosium ions (Dy^{3+}) have attracted significant attention since dysprosium-doped phosphors can be used in fluorescent lamps as a tricolor component and single-phase full-color phosphor in pc-LEDs [17]. Under n-UV excitation, there are generally three consistent bands in the visible region, including blue (470–500 nm), yellow (570–600 nm), and feeble red (670 nm) emissions, which are achieved when Dy^{3+} ions are incorporated in wide-band-gap host materials. These bands are associated with the hypersensitive electric dipole (ED) $^4F_{9/2} \rightarrow {}^6H_{15/2,\,13/2}$ transition and optical $^4F_{9/2} \rightarrow {}^6H_{11/2}$ transition in Dy^{3+} ions [18,19].

One strategy to achieve white light emission is adjusting the ratio of yellow to blue emission intensity, which reflects the coordination surroundings of the Dy^{3+} ion. Doping Dy^{3+} into an appropriate host is another strategy to obtain potential candidates for industrial applications [20]. In the present work, a simple and inexpensive phosphate host matrix and a suitable single RE dopant (Dy^{3+}) ion were investigated for their suitability in single-phase emission in the white light region. To the best of our knowledge, the optical properties of $LiNa_{3\text{-}x}P_2O_7$: xDy^{3+} phosphor has not been reported previously. The surface chemical composition of the elements in the phosphors was studied in detail by X-ray photoelectron spectroscopy.

2. Experimental

2.1. Synthesis

Polycrystalline powders of $LiNa_{3\text{-}x}Dy_xP_2O_7$ (x = 0, 0.05, 0.07, 0.09, and 0.11) were prepared by a solid-state reaction method. The materials were synthesized using the same experimental conditions as those in a recently published study [21]. In brief, analytical reagent-grade high-purity (99.99%) starting materials of Li_2CO_3, Na_2CO_3, $NH_4H_2PO_4$, and Dy_2O_3 were purchased (Sigma–Aldrich, USA) and used without further purification. To obtain homogeneity, stoichiometric amounts of reactive mixtures were finely ground in an agate mortar for 1 h. Each of the mixtures was placed in a separate silica crucible and gradually heated in a muffle furnace from room temperature (RT) to 400 °C for 4 h. This process eliminates the residual water, CO_2, and NH_3 from the mixtures. The samples were re-ground after cooling down to RT and then sintered at 540 °C for 12 h with several intermediate grindings. Finally, the samples were furnace cooled, ground again, and used for characterization.

2.2. Characterization

X-ray diffraction (XRD) patterns were collected using an X-ray diffractometer (PANalytical X'Pert PRO, USA) in a 2θ range of 10 to 70° with *Cu* K_α radiation at a wavelength of $\lambda = 1.5405$ Å. Attenuated total reflectance (ATR) - Fourier transform infrared (FTIR) spectra were recorded in the wavenumber range of 4000 to 400 cm^{-1} on a Perkin–Elmer (Bruker) IR spectrometer.

X-ray photoelectron spectroscopy (XPS) analysis was performed on an X-ray photoelectron spectrometer (K-alpha, Thermo Scientific, USA) using *Al* K_α X-ray radiation (1486.6 eV). All experiments were performed at analyzing chamber pressure of 1.8×10^{-8} mbar using pass energies of 160 and 30 eV and step sizes of 1 eV and 0.1 eV for the low and high-resolution spectra, respectively. Prior to measurements, the XPS instrument work function was calibrated with the standard Au $4f_{7/2}$ metallic binding energy (83.9 eV) and the spectrometer dispersion is adjusted to metallic Cu $2p_{3/2}$ binding energy (932.6 eV). The data were recorded and processed using the commercial software Avantage (Version 5.932, Thermo Scientific, USA). The charge shift corrections of the binding energies were adjusted relative to the carbon (C 1s = 284.8 eV) from hydrocarbons adsorbed on the surface of sample. Each core level spectrum was first fitted with a Shirley-type background and then deconvoluted into various components using GL30 (a mixture of Gaussian (70%) and Lorentzian (30%)) in Avantage. In the process of deconvolution of a signal, the full-width at half-maximum (FWHM) of each elemental spectrum was kept at similar value for different contributions.

The morphology of the sample was analyzed using a field-emission scanning electron microscope (FE-SEM) (S-4200, Hitachi, Japan). UV–Vis diffuse reflectance spectra (DRS) were recorded on a UV–Vis–NIR spectrophotometer (Jobin Varian Cary 5000, USA). The reflectance was measured in the range of 800 to 200 nm using polytetrafluoroethylene (PTFE) as a standard. Photoluminescence (PL) emission and excitation (PLE) spectra were recorded using a fluorescence spectrophotometer (Jobin Vyon Fluorolog–3, USA) with a xenon lamp as an excitation source. All the measurements were recorded at RT.

3. Results and discussion

3.1. X-ray diffraction analysis

The phase purity of the prepared pyrophosphate $LiNa_3P_2O_7$:Dy^{3+} phosphors were characterized by powder XRD analysis. The XRD patterns of the Dy-doped $LiNa_3P_2O_7$ samples are shown in Fig. 1. The dominant reflections of all the samples were well indexed with the host structure ($LiNa_3P_2O_7$) recently reported by Shi et al. [22] as well as the Inorganic Crystal Structure Data (ICSD: 424375). There were no other impurities in the patterns, indicating purity of the synthesized powders.

A closer look at the figure indicates that the predominant XRD peak positions are shifted toward a higher 2θ angle with increasing dopant concentration. In general, distortion of the XRD peaks from their mean position could be influenced by many factors, such as

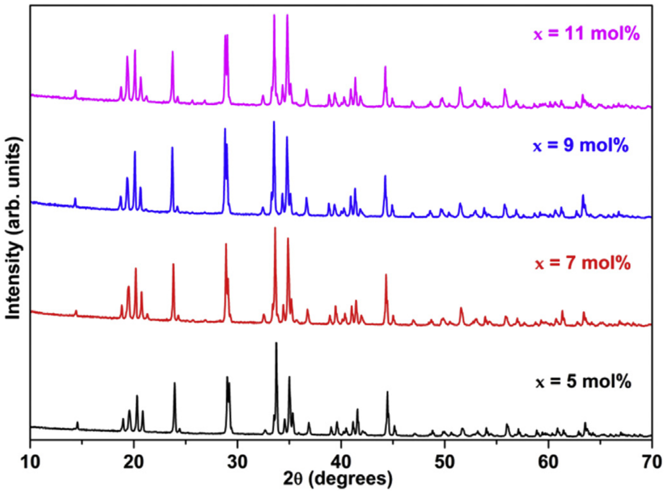

Fig. 1. XRD patterns of $LiNa_3P_2O_7$:Dy^{3+} phosphor (Dy^{3+} = 5–11 mol%).